

13. E. R. Gardner, T. L. Markin, R. S. Street, *J. Inorg. Nucl. Chem.* **27**, 541 (1965).
14. J. M. Haschke, T. H. Allen, J. L. Stakebake, *J. Alloys Compd.* **243**, 23 (1996).
15. J. M. Haschke and T. E. Ricketts, *J. Alloys Compd.* **252**, 148 (1997).
16. J. M. Haschke, A. E. Hodges, G. E. Bixby, R. L. Lucas, *Rep. RFP-3476* (Rocky Flats Plant, Golden, CO, 1983).
17. J. M. Haschke, in *Transuranium Elements: A Half Century*, L. R. Morss and J. Fuger, Eds. (American Chemical Society, Washington, DC, 1992), pp. 416–425.
18. C. A. Colmenares, *Prog. Solid State Chem.* **9**, 139 (1975).
19. L. A. Morales and A. C. Lawson, unpublished data.
20. M. McD. Baker, L. N. Ness, S. Orman, *Trans. Faraday Soc.* **62**, 2525 (1966).
21. C. E. Holley *et al.*, Proceedings of the Second United Nations International Conference on the Peaceful Uses of Atomic Energy, Geneva, Switzerland, 1–13 September 1958 (United Nations, Geneva, 1958), vol. 6, pp. 215–220.
22. J. M. Haschke and J. C. Martz, in *Encyclopedia of Environmental Analysis and Remediation*, R. A. Meyers, Ed. (Wiley, New York, 1998), vol. 6, pp. 3740–3755.
23. R. C. Dahlman, E. A. Bondietti, L. D. Eyeman, in *Actinides in the Environment*, A. M. Friedman, Ed. (American Chemical Society Symposium. Series No. 35, Washington, DC, 1976), pp. 47–80.
24. A. B. Kersting *et al.*, *Nature* **397**, 56 (1999).
25. This work was performed under U.S. Department of Energy Contract W-7405-ENG-36.

28 September 1999; accepted 18 November 1999

Communication Through a Diffusive Medium: Coherence and Capacity

Aris L. Moustakas,^{1*} Harold U. Baranger,^{1,2} Leon Balents,^{1,3}
Anirvan M. Sengupta,¹ Steven H. Simon¹

Coherent wave propagation in disordered media gives rise to many fascinating phenomena as diverse as universal conductance fluctuations in mesoscopic metals and speckle patterns in light scattering. Here, the theory of electromagnetic wave propagation in diffusive media is combined with information theory to show how interference affects the information transmission rate between antenna arrays. Nontrivial dependencies of the information capacity on the nature of the antenna arrays are found, such as the dimensionality of the arrays and their direction with respect to the local scattering medium. This approach provides a physical picture for understanding the importance of scattering in the transfer of information through wireless communications.

The ongoing communications revolution has motivated researchers to look for novel ways to transmit information (1, 2). One recent development (3, 4) is the suggestion that, contrary to long-held beliefs, random scattering of microwave or radio signals may enhance the amount of information that can be transmitted on a particular channel. Prompted by this suggestion, we introduce a realistic physical model for a scattering environment and analytically evaluate the amount of information that can be transmitted between two antenna arrays for a number of example cases. On the one hand, this lays a new foundation for complex microwave signal modeling, an important task in a world with ever-increasing demand for wireless communication, and on the other, it introduces a new arena for physicists to test ideas concerning disordered media.

From information theory (5), the capacity of a channel between a transmitter and a receiver, that is, the maximum rate of information transfer at a given frequency, can be described in terms of the average power

of the signal S and the noise N at the receiver: $C = \log_2(1 + S/N)$. More generally (2), the communication channel connecting several transmitters and receivers is described by a matrix $G_{i\alpha}$ giving the amplitude of the received signal α due to transmitter i . The information carried by the channel can be characterized by using several quantities, such as the capacity or mutual information, which are typically functionals of the matrix G , which must be known in order to predict these quantities. Often G cannot be predicted for actual systems, such as wireless communication networks or optical fibers, because of the complicated scattering and interference of waves that are involved. It is crucial, therefore, to develop physical models for the signal propagation, because it is only through such models that one can understand the real effects of scattering and interference on the amount of information that can be communicated.

In many cases, only partial information is available for prediction; in these situations, one has only a statistical description of G . Instead of making assumptions about G directly, which is the usual procedure in information theory, we introduce statistical models for the physical environment from which we derive the properties of G . The advantage of this procedure is that simple physical models can yield very nontrivial properties of G .

Statistical descriptions of the environment have been quite successful in the physics of disordered media (6–9). The simplest of these is diffusive propagation. In our case of electromagnetic propagation in the context of wireless communication, diffusion is known to work well in various circumstances (10), and simple extensions seem relevant for many others. From a diffusive approach, one finds the moments of the distribution of G . These will enable us to calculate information-theoretic quantities (for example, the capacity) using a replica field theory approach to random matrix theory (11). Implicit in this approach is the assumption that the full distribution of G is sampled, which is realistic in many real-world situations where the environment is changing. However, when the number of antennas is large, many quantities of interest become strongly peaked around their average and this assumption can be relaxed.

In a statistical description, the scattering of the signal is characterized by the mean-free path, ℓ , corresponding roughly to the distance between scattering events. When ℓ is large compared to the wavelength λ but small compared to the distance d between the two arrays, the wave propagation becomes diffusive (8, 9). This has been analyzed previously in the context of electron diffusion in metals (6, 7) and light propagation in solids (8, 12). In the case of wireless propagation, with signals in the 2-GHz region, $\lambda \sim 10$ to 15 cm, while ℓ is on the order of meters for indoors and tens of meters for outdoors propagation, so diffusion is applicable.

In the diffusive regime $\lambda \ll \ell$, to leading order in λ/ℓ , only the quadratic correlations $\langle G_{i\alpha} G_{j\beta}^* \rangle$ are nonnegligible and therefore describe the system, where the brackets represent an average over realizations of the disorder. Higher cumulants of G are of higher order in λ/ℓ . Therefore, the distribution of G is Gaussian with zero average (6–9). The leading term in $\langle G_{i\alpha} G_{j\beta}^* \rangle$ is evaluated by a summation of so-called ladder diagrams (8) corresponding to processes in $\langle G_{i\alpha} G_{j\beta}^* \rangle$ where the waves from antennas i to α and from j to β propagate through the scattering medium along identical paths except for segments of order ℓ at each end.

In several realistic situations discussed be-

¹Bell Labs, Lucent Technologies, 700 Mountain Avenue, Murray Hill, NJ 07974, USA. ²Department of Physics, Duke University, Durham, NC 27708–0305, USA. ³Department of Physics, University of California, Santa Barbara, CA 93106, USA.

*To whom correspondence should be addressed. E-mail: arislm@physics.bell-labs.com

low, the correlations take a particularly simple form:

$$\langle G_{i\alpha} G_{j\beta}^* \rangle = R_{\alpha\beta} \frac{S}{n_T} T_{ij} \quad (1)$$

Here $R_{\alpha\beta}$ and T_{ij} are matrices describing the correlations of the receiving and transmitting antennas, respectively, and $S = \text{Tr}\{GG^\dagger\}/n_R$ is the average power received at each of n_R receivers assuming independent signals from each of n_T transmitters. R and T are normalized such that $\text{Tr}\{T\} = n_T$ and $\text{Tr}\{R\} = n_R$. The factorization in Eq. 1 of the receiver and transmitter information reflects the dominance of the ladder terms: Only the segments near the antennas contribute a net phase, so only local information about the antennas is relevant. Furthermore, under general circumstances, T can be expressed in terms of the response $\chi_i(\hat{\mathbf{k}}, \hat{\mathbf{e}})$ of antenna i to an incoming plane wave in direction $\hat{\mathbf{k}}$ with polarization $\hat{\mathbf{e}}$ and a weight function $w(\hat{\mathbf{k}}, \hat{\mathbf{e}})$ giving the fraction of incident power in that direction with that polarization:

$$T_{ij} \propto \int d\hat{\mathbf{k}} \sum_{\hat{\mathbf{e}}} w(\hat{\mathbf{k}}, \hat{\mathbf{e}}) \chi_i(\hat{\mathbf{k}}, \hat{\mathbf{e}}) \chi_j^*(\hat{\mathbf{k}}, \hat{\mathbf{e}}) \quad (2)$$

R is defined similarly.

Having summarized the coherent diffusion results that we will need, we now turn to considering information-theoretic quantities. While there are many such quantities that one could study with the diffusive techniques outlined above, for concreteness we focus on a problem of relevance to wireless communication applications (2-4, 13, 14). We assume that (i) the receiver knows G , but the transmitter does not; (ii) the noise at each receiving antenna has the same power N and is Gaussian uncorrelated; and (iii) after a long time, the entire space of possible G matrices is explored as the environment changes, subject to the statistical properties of Eq. 1. Under these circumstances, the maximum time-averaged information transfer rate is given by the so-called capacity, formally defined in (15), given by (2-4)

$$C = \max_Q \left\langle \text{Tr} \left\{ \log_2 \left[I_{n_R} + \frac{1}{N} G Q G^\dagger \right] \right\} \right\rangle \quad (3)$$

where I_{n_R} is the $n_R \times n_R$ unit matrix and Q is the nonnegative-definite $n_T \times n_T$ covariance matrix describing the correlations between the signals from the transmitter antennas. Here, the angled brackets again indicate an average over realizations of G with correlations defined by Eq. 1. With the normalization of G given above, the constraint on the maximum power transmitted yields the condition $\text{Tr}\{Q\} \leq n_T$. For a fixed covariance Q , the maximum information transfer rate is given by the same expression only without the \max_Q in front. Maximization over Q then

gives the capacity of the channel.

The assumptions (i) to (iii) given above are appropriate for certain real-world systems, and have been previously studied (3, 4). Assumption (i) is appropriate if the transmitter occasionally sends known signals so the receiver can determine G , and if G changes slowly enough that the channel needs to be probed only very occasionally. We also assume that the receiver cannot send information about G back to the transmitter. Assumption (iii), while necessary to make Eq. 3 formally correct, is not too important in practice for systems with a large number of antennas where the maximum information transfer rate for a given Q is strongly peaked about its average value (3, 16).

An important implication of Eq. 3, recently pointed out in (3, 4), is that if the environment is sufficiently multipath, the capacity increases linearly with the number of antennas even when the total transmitted power is fixed, greatly exceeding the capacity of line-of-sight propagation. This result may seem surprising because scattering may reduce the received signal. However, the scattering also produces many independent paths that interfere at both the transmitter and receiver. This interference can be exploited by placing several antennas at both ends in order to increase the capacity. We now illustrate this dramatic result with a simple example.

Consider the case of two antennas at each end and assume that a single scatterer (a mirror) is at some point between the two arrays (Fig. 1). Here and throughout this report the Fresnel limit will be assumed: The size of the transmitter and receiver arrays is much smaller than $\sqrt{\lambda d}$. In the absence of scattering there is only line-of-sight propagation. Due to the small effective aperture of the receiving array, it is impossible to resolve the different transmitting antennas. Thus, the capacity is the same as if there were only one transmitter and one receiver antenna, except that the noise level is reduced by a factor of 2 because it is averaged over two receivers. Mathematically, this corresponds to G being a rank one matrix, indicating only one channel of communication. Including the mirror, the signal received is now the sum of the direct line-of-sight and the scattered amplitudes. If the two incoming waves are at very different angles, then the aperture of the receiving array is sufficient to resolve the two waves separately. It is thus possible to distinguish the two signals originating from the two transmitters. Now, G is of rank two, so there are two nonzero terms (two channels) in Eq. 3, roughly doubling the capacity.

Foschini and Gans argue (3) that for many scatterers, it is possible for G to become of full rank (14) such that the capacity is proportional to the number of antennas. An increase in capacity can thus be obtained even

if S/N is reduced by scattering because this latter effect reduces the capacity only logarithmically. In order to derive their results, they assume that G is a random matrix with completely uncorrelated elements. Their situation (fully uncorrelated matrix elements) corresponds to R and T being identity matrices in Eq. 1 so that the optimal Q in Eq. 3 is identity also. This yields, in fact, an upper bound on the capacity that can be realized only in very special circumstances.

We now generalize the results of Foschini and Gans (3) to situations with nontrivial correlations (R and T not identity) that actually occur in real systems. The capacity (15) defined by Eq. 3 with such nontrivial correlations has not been considered previously. These correlations (nontrivial T and R) indicate some redundancy in both the transmitter and receiver arrays, thus reducing the capacity.

Surprisingly, we find that the capacity (Eq. 3) can be evaluated analytically for a large number of antennas by using replica field theory extensively applied in statistical physics (11) once T and R are known (that is, given $\langle G_{i\alpha} G_{j\beta}^* \rangle$). The result of this approach is a set of algebraic equations for the capacity in terms of the eigenvalues of R and T , which will be described in detail elsewhere. In contrast, attempting to evaluate Eq. 3 numerically by generating realizations of G with appropriate covariance would be quite difficult because one must then maximize over Q .

We now analyze illustrative situations involving scattering media. The simplest case is when scalar waves are considered and the antennas are deep inside a uniform and isotropic scattering medium with a mean free path that is large compared to the size of the arrays. In addition, if we assume that the antennas are ideal, making a perfect measurement of the field at one point without distorting it in any way, then $\chi_i(\hat{\mathbf{k}}) = \exp(ik_0 \hat{\mathbf{k}} \cdot \mathbf{r}_i)$ (no $\hat{\mathbf{e}}$ appears for scalar waves). Due to isot-

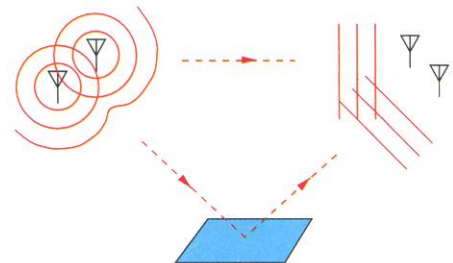


Fig. 1. Transmitter and receiver antenna arrays in the presence of a single scatterer (mirror). Electromagnetic waves interfere at both transmitter and receiver antennas. The presence of the scatterer introduces an additional path of wave propagation between the two arrays and thereby additional interference at both ends. As a result, the receiver can resolve the individual signals from the two different transmitting antennas.

copy, $w(\hat{\mathbf{k}}) = 1$, and thus using Eq. 2, we obtain $T_{ij} = f(k_0|\mathbf{r}_i - \mathbf{r}_j|)$ and $R_{\alpha\beta} = f(k_0|\mathbf{r}_\alpha - \mathbf{r}_\beta|)$ with $f(x) = \sin(x)/x$ where $k_0 = 2\pi/\lambda$ and \mathbf{r}_i are the antenna positions. When the antennas are separated by multiples of $\lambda/2$, all antennas of each array are on a straight line, there are no correlations, and R and T are unit matrices as assumed by Foschini and Gans. Any other configuration has nontrivial correlations and therefore lower capacity.

An important consequence of the form of the correlation matrices is the scaling of the capacity with the number of antennas. In the

limit of a large periodic array of antennas, the eigenvectors of T and R are plane-waves (by Bloch's theorem) so one can find the eigenvalues analytically. When antennas are placed on a one- or two-dimensional array (Fig. 2), the capacity is proportional to the antenna number. However, when they are placed in a three-dimensional array, the capacity scales as $n^{2/3}$ up to a logarithm, not linearly. The model of a scattering medium discussed above gives an intuitive interpretation of this result: A finite thickness of antennas on the surface is sufficient to resolve the incoming waves from the transmitting

antennas; additional antennas in the interior are redundant. Therefore the optimal Q is such that less power is transmitted from these interior antennas.

As a second example we consider ideal dipole antennas and vector electromagnetic waves. The average power propagating is the same as for scalar waves, because vectorial diffusion (nonzero spin) decays exponentially (12). The correlation matrices are now given by using $\chi_i(\hat{\mathbf{k}}, \hat{\epsilon}) = (\hat{\mathbf{p}}_i \cdot \hat{\epsilon}) \exp(ik_0\hat{\mathbf{k}} \cdot \mathbf{r}_i)$ in Eq. 2, where $\hat{\mathbf{p}}_i$ is the polarization of antenna i . From the resulting expression, one finds that if antennas are positioned on a straight line with polarization at an angle $\theta = 54.73^\circ$ ($\cos^2\theta = \frac{1}{3}$) with respect to that line, the correlations again vanish when antenna separations are multiples of $\lambda/2$. In this case, then, the ideal situation of Foschini and Gans is again realized; however, for any other angle, correlations play a role even if the antennas are separated by half wavelengths.

The simplest case in which the geometry of the environment is taken into account is a half-infinite diffusive three-dimensional region without any scattering in the other half space (Fig. 3). This is a first approximation to modeling electromagnetic propagation in a city of high-rise buildings. When either of the arrays is close to the surface of the diffusive region, the correlations between antennas become qualitatively different. Specifically, when one antenna array is outside while the other is deep inside the scattering medium, $w(\hat{\mathbf{k}}) = (\hat{\mathbf{k}} \cdot \hat{\mathbf{z}})\Theta(\hat{\mathbf{k}} \cdot \hat{\mathbf{z}})$ for the outside antenna array (for either scalar or vector waves) where $\hat{\mathbf{z}}$ is the normal to the interface and Θ is the Heaviside step function. Surprisingly, the maximum capacity is achieved by pointing the transmitter directly into the diffusive medium rather than at the receiver!

We close by pointing out several simple extensions that make these methods applicable to a wide variety of realistic situations. First, more realistic modeling of the scattering medium could take into account scatterers that are not small compared to the wavelength. A concrete example is the scattering off walls inside a building where the scattering is highly anisotropic (10). This case can be analyzed within our framework; however, the correlations no longer have the simple factorized form of Eq. 1.

Second, more realistic antennas can be treated by simply inserting appropriate functions $\chi_i(\hat{\mathbf{k}}, \hat{\epsilon})$ in Eq. 2. Even for nontrivial antennas, these functions can be either determined numerically or measured experimentally. In this way, both practical antenna designs and the effects of antenna interactions can be included.

Finally, we can consider the case where the transmitter also has knowledge of G . In this case, the capacity will be greater. Here, the averaging over G occurs after optimiz-

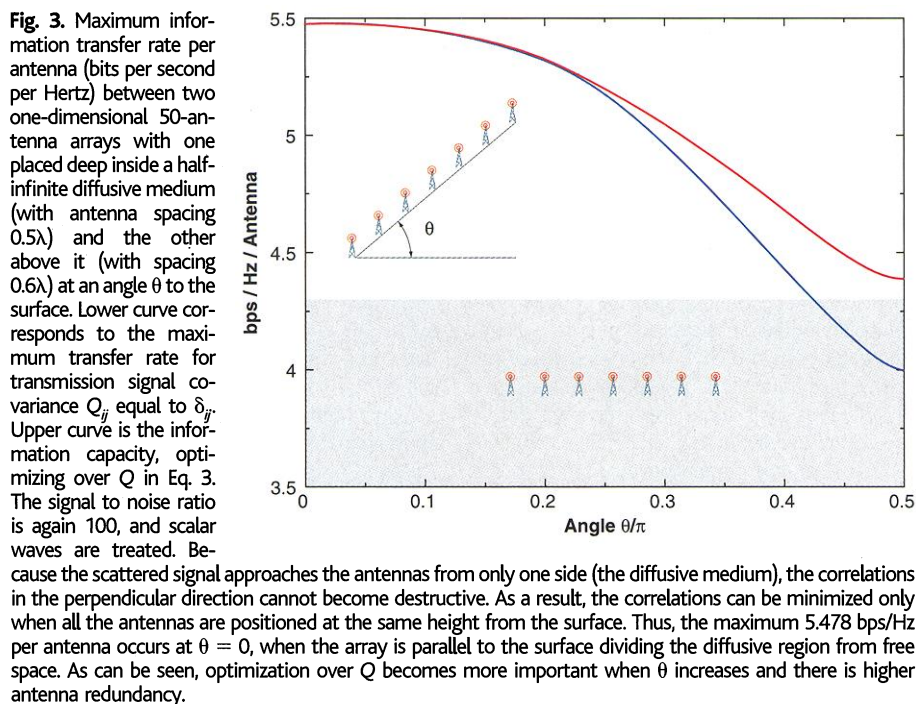
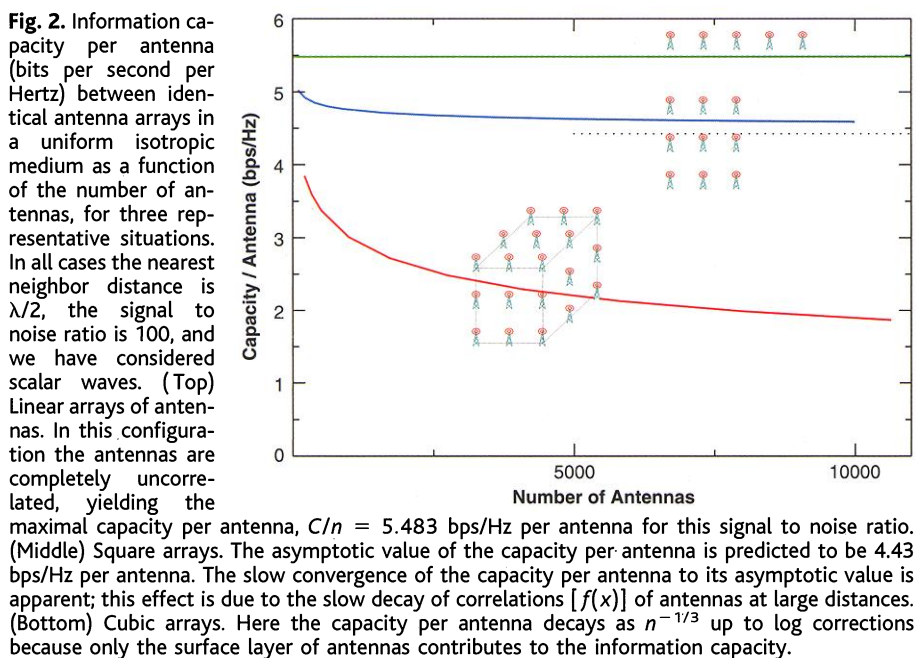


Fig. 3. Maximum information transfer rate per antenna (bits per second per Hertz) between two one-dimensional 50-antenna arrays with one placed deep inside a half-infinite diffusive medium (with antenna spacing 0.5λ) and the other above it (with spacing 0.6λ) at an angle θ to the surface. Lower curve corresponds to the maximum transfer rate for transmission signal covariance Q_{ij} equal to δ_{ij} . Upper curve is the information capacity, optimizing over Q in Eq. 3. The signal to noise ratio is again 100, and scalar waves are treated. Because the scattered signal approaches the antennas from only one side (the diffusive medium), the correlations in the perpendicular direction cannot become destructive. As a result, the correlations can be minimized only when all the antennas are positioned at the same height from the surface. Thus, the maximum 5.478 bps/Hz per antenna occurs at $\theta = 0$, when the array is parallel to the surface dividing the diffusive region from free space. As can be seen, optimization over Q becomes more important when θ increases and there is higher antenna redundancy.

ing over Q , a process known as “water-filling” (2). This case can also be handled within our framework.

References and Notes

1. T. S. Rappaport, *Wireless Communications, Principles and Practice* (Prentice-Hall, Englewood Cliffs, NJ, 1996).
2. T. M. Cover and J. A. Thomas, *Elements of Information Theory* (Wiley, New York, 1991); S. Kullback, *Information Theory and Statistics* (Wiley, New York, 1959).
3. G. J. Foschini and M. Gans, *Wireless Personal Commun.* **6**, 311 (1998).
4. I. E. Telatar, *Eur. Trans. Telecommun.*, in press.
5. C. E. Shannon, *Bell Syst. Tech. J.* **27**, 379, 623 (1948).
6. B. L. Altshuler, P. A. Lee, R. A. Webb, Eds., *Mesoscopic Phenomena in Solids* (North-Holland, New York, 1991).

7. E. Akkermans, G. Montambaux, J.-L. Pichard, J. Zinn-Justin, Eds., *Mesoscopic Quantum Physics* (Elsevier, New York, 1995).
8. M. J. Stephen, in (6), pp. 81–106.
9. M. C. W. van Rossum and Th. M. Nieuwenhuizen, *Rev. Mod. Phys.* **71**, 313 (1999).
10. D. Ullmo and H. U. Baranger, *IEEE Trans. Veh. Technol.* **48**, 947 (1999).
11. A. M. Sengupta and P. P. Mitra, *Phys. Rev. E* **60**, 3389 (1999).
12. M. J. Stephen and G. Cwilich, *Phys. Rev. B* **34**, 7564 (1986).
13. E. Biglieri, J. Proakis, S. Shamai (Shitz), *IEEE Trans. Inf. Theory* **44**, 2619 (1998).
14. J. G. Foschini, M. Gans, D. Shiu, J. M. Kahn, *IEEE Trans. Commun.*, in press.
15. Formally, we pose this information theory problem as follows. The received signal vector is $y =$

$Gx + \eta$ where x is the transmitted vector and η is the noise vector. Thus, the channel is defined by $p(\{G,y\}|x) = p(G)p(y|G,x)$ where $p(G) \propto \exp[-n_r/2S \text{Tr}(GT^{-1}G^*R^{-1})]$ gives G the proper statistics as defined by Eq. 1, and $p(y|G,x) \propto \exp(-1/2N|y - Gx|^2)$ describes independent noise of average power N in each component of η . The capacity as shown in Eq. 3 is then the mutual information $I(\{G,y\};x)$ maximized over all possible $p(x)$ transmitted.

16. A. M. Sengupta and P. P. Mitra, Bell Labs Memo 11111-990318-05.

17. We thank G. J. Foschini, M. Gans, and B. I. Halperin for illuminating discussions.

26 August 1999; accepted 22 November 1999

Direct Observation of Dynamical Heterogeneities in Colloidal Hard-Sphere Suspensions

Willem K. Kegels¹ and Alfons van Blaaderen^{1,2}

The real-space dynamics in a model system of colloidal hard spheres was studied by means of time-resolved fluorescence confocal scanning microscopy. Direct experimental evidence for the presence of dynamical heterogeneities in a dense liquid was obtained from an analysis of particle trajectories in two-dimensional slices of the bulk sample. These heterogeneities manifest themselves as a non-Gaussian probability distribution of particle displacements and also affect the onset of long-time diffusive behavior.

Many liquids can be transformed into a glass, a solid phase without long-range positional order, by cooling them rapidly below their freezing temperature (1, 2). The change in molecular relaxation processes upon approaching the glass transition continues to be the subject of much experimental and theoretical work [for a recent review see (3)]. This change reflects the increase of correlations of the particle movements upon approaching the glass transition. However, such relaxation processes are not only of interest from a fundamental viewpoint: The nature and time scales of these processes determine the (kinetic) stability of a glass (relative to the crystalline state) and its mechanical properties.

An important observation in many molecular glass-forming liquids is a nonexponential decay of (ensemble-averaged) time correlation functions [see (4) and references therein]. Both computer simulation and indirect experimental evidence [for example, (5)]

suggest that a superposition of different relaxation processes, or dynamic heterogeneity, underlies this nonexponential behavior. Molecular dynamics simulations have given direct evidence for dynamical heterogeneities (6, 7), and a Monte Carlo simulation of hard spheres, which focused on three-time correlations of single particles (8), also indicates (albeit indirectly) that dynamical heterogeneities occur.

In recent studies on colloidal systems, the dynamics of tracer particles was investigated by optical microscopy (9) and by dynamic light scattering (10). In both studies, deviations of the displacement distribution function from Gaussian behavior were observed. However, dynamical heterogeneities were not observed directly in these experiments. Colloidal systems may be regarded as collections of “superatoms” in which the interaction potential can be tailored (11), for example, by changing the solvent quality. During the past decade, they have also been used as model systems to study the glass transition (12).

Here, we investigated the nature of dynamical heterogeneities for the simplest possible experimental (model) system of interacting particles: hard colloidal spheres. We used fluorescent confocal scanning laser mi-

croscopy to obtain time series of digital images of the colloidal particles, in slices in the bulk of the sample. The data from these images enable us to address the question of how these heterogeneities are manifested in (real-space) correlation functions.

Colloidal particles that could be observed directly by microscopy were developed in our laboratory. They are of a core-shell nature and can be matched for (mass) density and for refractive index (13). The particles consist of a core of silica with a fluorescent dye (fluorescein isothiocyanate) (14), 450 nm in diameter, covered with a large shell of polymethylmethacrylate (PMMA) with a steric stabilizing layer (~10 nm thick) of 12-polyhydroxystearic acid (PHS) that is covalently linked to the PMMA (15, 16). The particles were dispersed in a mixture of tetralin, decalin, and carbon tetrachloride in which the particles are almost matched with respect to refractive index and density. In this solvent mixture, the diameter of the particles is 1.40 μm and the size polydispersity is ~6%. This relatively large polydispersity inhibits crystallization (above the freezing volume fraction of 0.494) considerably: Months elapsed before crystallites formed. From the location of the coexisting fluid-crystal volume fractions and from light scattering studies, it could be concluded that the particles behave as hard spheres. This conclusion is corroborated by the shape of the pair correlation or radial distribution function (see below) and by the independence of the location of the first peak on the volume fraction of the spheres.

The volume fraction of the particles where no movement was observed (except for a few “rattlers,” trapped particles that are not immobilized) was set at 0.66. This density coincides with the volume fraction at random close packing of 6% polydisperse hard spheres (17). All volume fractions are defined relative to this point. Because of the core-shell character of the particles, time-dependent coordinates of their centers could be obtained with high accuracy using proce-

¹Van't Hoff Laboratory for Physical and Colloid Chemistry, Debye Institute, Utrecht University, Padualaan 8, 3584 CH Utrecht, Netherlands. ²Institute for Atomic and Molecular Physics, Stichting voor Fundamenteel Onderzoek der Materie (FOM), Kruislaan 407, 1098 SJ Amsterdam, Netherlands.